International Journal of Bifurcation and Chaos, Vol. 29, No. 2 (2019) 1950021 (16 pages)

DOI: 10.1142/S0218127419500214

Categories of Conservative Flows

Sajad Jafari*
Biomedical Engineering Department,
Amirkabir University of Technology,
Tehran 15875-4413, Iran
sajadjafari83@gmail.com

Julien C. Sprott
Department of Physics, University of Wisconsin,
Madison, WI 53706, USA

Soroush Dehghan
Biomedical Engineering Department,
Amirkabir University of Technology,
Tehran 15875-4413, Iran

Received August 10, 2018

In this note, we define four main categories of conservative flows: (a) those in which the dissipation is identically zero, (b) those in which the dissipation depends on the state of the system and is zero on average as a consequence of the orbits being bounded, (c) those in which the dissipation depends on the state of the system and is zero on average, but for which the orbit need not be bounded and a different proof is required, and (d) those in which the dissipation depends on the initial conditions and cannot be determined from the equations alone. We introduce a new 3D conservative jerk flow to serve as an example of the first two categories and show what might be the simplest examples for each category. Also, we categorize some of the existing known systems according to these definitions.

Keywords: Conservative; chaotic flows; divergence; Hamiltonian.

1. Introduction

Conservative dynamical systems are ones in which the phase space volume is conserved and the flow is incompressible according to Liouville's theorem [Lichtenberg & Lieberman, 2013]. Such systems have a long history rooted in the study of celestial mechanics and were formalized by Euler, Lagrange, Hamilton, Jacobi, and others two centuries ago. Although they do not have attractors, conservative systems can exhibit different dynamical behaviors including chaos [Sprott, 2010].

A general dynamical system is given by

$$\begin{aligned} v_1 &= \dot{x}_1 = f_1(x_1, x_2, \ldots, x_n),\\ v_2 &= \dot{x}_2 = f_2(x_1, x_2, \ldots, x_n),\\ &\vdots\\ v_n &= \dot{x}_n = f_n(x_1, x_2, \ldots, x_n), \end{aligned} \tag{1}$$

where $x_1, x_2, \ldots, x_n$ are dynamical (state) variables, $v_1, v_2, \ldots, v_n$ are the time derivatives of the state

*Author for correspondence

(velocities), and $f_1(X), f_2(X), \ldots, f_n(X)$ are the evolution equations (velocity vectors). If the divergence (trace of the Jacobian) of a system is identically zero for all values of the state, then the system is conservative, while if the trace is constant and nonzero, it is not conservative. If the divergence is negative, the system is dissipative, and if it is positive, the system is unbounded. However, the divergence sometimes depends on the state, in which case the time-average of the divergence along the trajectory determines whether the system is conservative or not (by being zero or nonzero). Such systems are globally conservative but have regions of state space that are dissipative and other regions that are anti-dissipative. Heidel and Zhang call such systems nonuniformly conservative [Heidel & Zhang, 2007].

In this note, we describe four different categories of conservative dynamical systems. Two of these categories (A and C) are well-known, while the other two (Categories B and D) are less familiar. We provide what may be the simplest examples for each of the four types in 3D systems with quadratic nonlinearities.

2. Four Categories of Conservative Flows

2.1. *Category A*

If the divergence (trace of the Jacobian) of a system is identically zero, then the system is conservative. All the many Hamiltonian systems that have been studied since the time of Newton are of this type. Such systems are $2N$-dimensional, where N is the number of degrees of freedom. However, it is also possible for three-dimensional systems to be conservative, and such cases are of special interest because they represent the simplest cases that can have chaotic solutions according to the Poincaré–Bendixson theorem.

Consider the following 3D jerk system, so-called because in a mechanical system, $\dot{z}$ would represent the time derivative of the acceleration:

$$\begin{aligned} \dot{x} &= y, \\ \dot{y} &= z, \\ \dot{z} &= x(1+x) - ay + byz. \end{aligned} \tag{2}$$

The local divergence is $(\frac{\partial \dot{x}}{\partial x} + \frac{\partial \dot{y}}{\partial y} + \frac{\partial \dot{z}}{\partial z} = by)$, and the system is uniformly conservative if $b = 0$, in which case all orbits are unbounded for less than about 1.6. Heidel and Zhang have proved that a system of this form cannot have chaotic solutions [Heidel & Zhang, 2007]. However, for larger values of a, there is a periodic orbit surrounded by a set of nested tori on which the orbits are quasi-periodic. For example, $a = 5$ gives the system

$$\dot{x} = y, \quad \dot{y} = z, \quad \dot{z} = x(1+x) - 5y \tag{3}$$

whose cross-section in the $z = 0$ plane for various initial conditions is shown in Fig. 1. The toroidal region is bounded by the two equilibria at $(-1, 0, 0)$ and $(0, 0, 0)$ shown as blue dots. The former equilibrium has eigenvalues $(-0.1923, 0.0962 \pm 2.2340i)$, and the latter has eigenvalues $(0.1923, -0.0962 \pm 2.2340i)$. Thus both equilibria are unstable saddle foci, and they lie on the boundary of the bounded region.

A typical torus with initial conditions $(-0.5, 1, 0)$ is shown in Fig. 2. For a conservative torus in 3D, all three Lyapunov exponents are zero: $(0, 0, 0)$. However, there is a local expansion and contraction of the flow as if it were contained in a pipe of varying diameter, causing the local value of the largest Lyapunov exponent to vary between about ± 2.3 with an average value that is accurately zero. This is shown in the plot using a red color to indicate regions where the local Lyapunov exponent is positive and blue where it is negative.

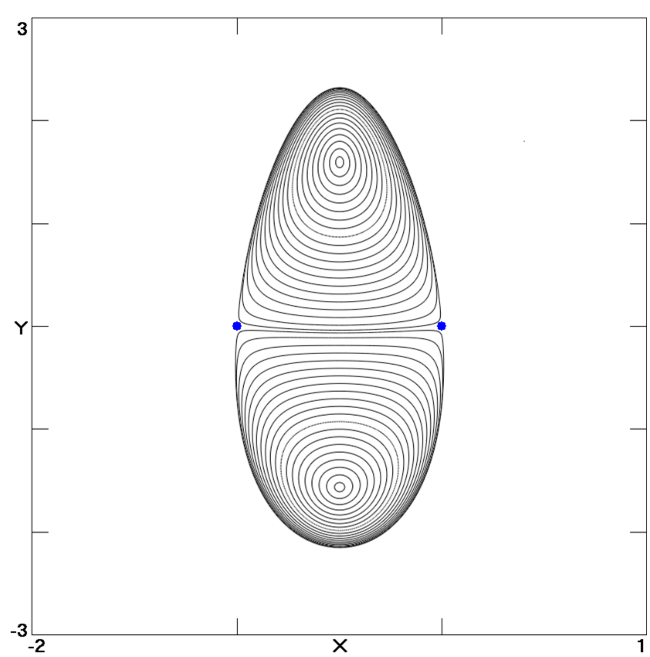

Fig. 1. Cross-section of the nested tori in the $z = 0$ plane for system (3). The toroidal region is bounded by the two equilibria at $(-1, 0, 0)$ and $(0, 0, 0)$ shown as blue dots, outside of which all orbits are unbounded.

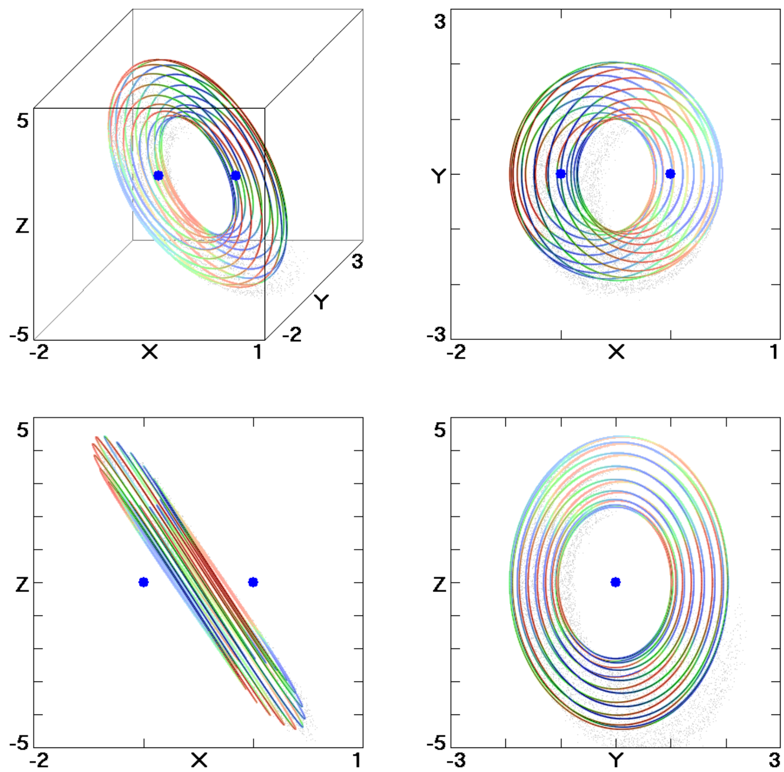

Fig. 2. Different projections of a typical torus for system (3) with initial conditions $(-0.5, 1, 0)$.

2.2. *Category B*

If Eq. (1) has a bounded solution, the average velocity ($v_{i_{\text{average}}} = \bar{v}_i = \frac{\Delta x_i}{\Delta t}$ of all the states should be zero. We denote the average value of a variable $S(t)$ as $\langle S(t)\rangle$ which is defined as $\langle S(t)\rangle = \lim_{t\to\infty} \frac{\int_{t_0}^{t} S(t)dt}{t-t_0}$. Using proof by contradiction, suppose that one of the variables (x_i) in Eq. (1) has a nonzero average velocity $\langle v_i\rangle = a \neq 0$. In this case, since $x_i(t) = \int_{t_0}^{t} v_i(t)dt \approx at + x_i(t_0)$ and $t \to \infty$, this variable drifts to infinity by the passage of time, and this is inconsistent with the assumption that the solutions are bounded.

Consider system (2) when $b \neq 0$. Then the average divergence is $\langle \frac{\partial \dot{x}}{\partial x} + \frac{\partial \dot{y}}{\partial y} + \frac{\partial \dot{z}}{\partial z}\rangle = b\langle y\rangle$. Since the average value of $\dot{x}$, $\dot{y}$, and $\dot{z}$ should be zero (as conditions for having a bounded solution), which means $\langle z\rangle = 0$, $\langle y\rangle = 0$, and $\langle x(1+x) - ay + byz\rangle = 0$, the divergence will be zero on average. An example of such a nonuniformly conservative system with $a = 5$ and $b = 1$ is

$$\dot{x} = y, \quad \dot{y} = z, \quad \dot{z} = x(1+x) - 5y + yz. \tag{4}$$

Like system (3), system (4) has quasi-periodic solutions, but apparently not chaotic ones. A cross-section of the nested tori in the $z = 0$ plane is shown in Fig. 3. The plot is just a distorted version of the one in Fig. 1. The equilibria and their eigenvalues are identical to those for system (3), and the dynamics are similar with a Lyapunov exponent spectrum of $(0, 0, 0)$ throughout the bounded region. However, the Lyapunov exponents converge slowly for orbits that pass near the equilibria, producing long-duration transient chaos.

A typical torus with initial conditions $(-0.5, 1, 0)$ as shown in Fig. 4 is just a slightly distorted version of Fig. 2. As before, the local largest Lyapunov exponent varies between about ± 4.6 with an average value that converges slowly to zero. Larger values of b cause further distortion of the tori until they are destroyed around $b = 3$ and all orbits are unbounded.

2.3. *Category C*

The oldest example of a nonuniformly conservative chaotic flow is the Sprott case A system [Sprott, 1994]:

$$\dot{x} = y, \quad \dot{y} = -x + yz, \quad \dot{z} = 1 - ay^2. \tag{5}$$

This is an important system since it is a special case of the Nosé–Hoover thermostatted oscillator [Posch *et al.*, 1986; Hoover, 1995] which models a

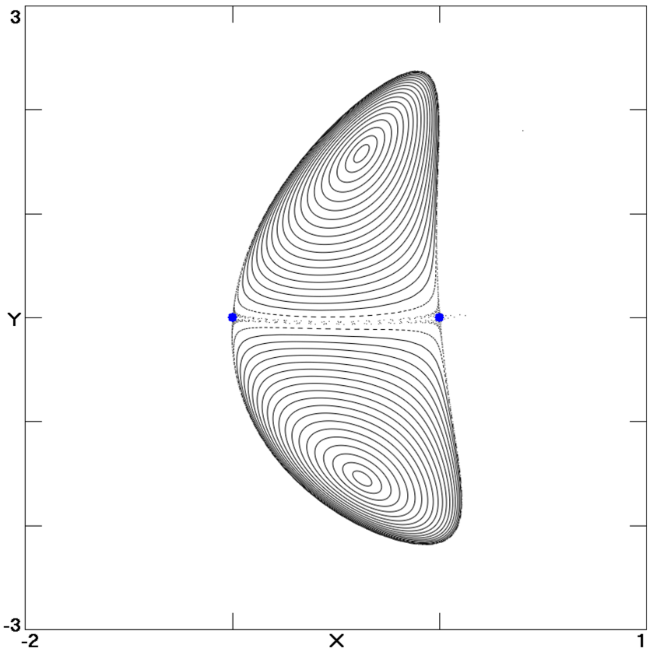

Fig. 3. Cross-section of the nested tori in the $z = 0$ plane for system (4). The toroidal region is bounded by the two equilibria at $(-1, 0, 0)$ and $(0, 0, 0)$ shown as blue dots, outside of which all orbits are unbounded.

simple harmonic oscillator in contact with an infinite heat bath with a temperature $\langle y^2 \rangle = 1/a$ and represents a starting point for molecular dynamic simulations. System (6) has solutions that lie on a nested set of intricate tori surrounded by a chaotic sea as shown in Fig. 5 for $a = 1$. The chaotic sea stretches to infinity but with a Gaussian measure, and orbits in the sea have Lyapunov exponents of $(0.0139, 0, -0.0139)$ and a Kaplan–Yorke dimension of 3.0. A typical torus with initial conditions $(0, 1, 0)$ surrounded by an orbit in the chaotic sea with initial conditions $(0, 5, 0)$ is shown in Fig. 6. The local largest Lyapunov exponent varies between about ± 1.2 on the torus and between about ± 4.0 for the portion of the chaotic orbit shown in the figure. The large variance of the local Lyapunov exponents is typical of chaotic systems and is one reason the Lyapunov exponents converge so slowly, and why it is often difficult to distinguish quasi-periodicity from weak chaos. The system is unbounded in the sense that orbits will eventually reach points arbitrarily far from the origin where the local Lyapunov exponent is enormous, but those orbits eventually

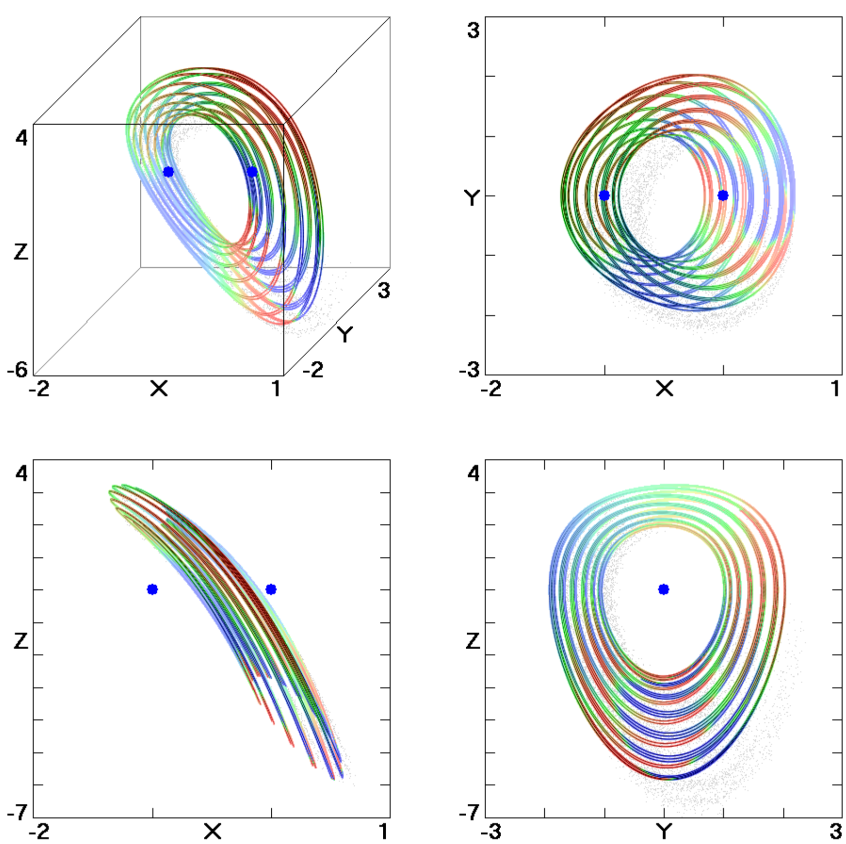

Fig. 4. Different projections of a typical torus for system (4) with initial conditions $(-0.5, 1, 0)$.

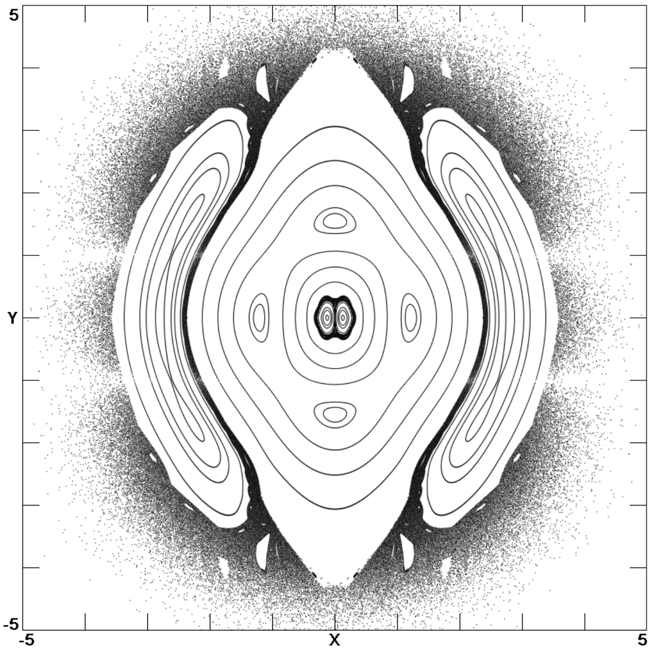

Fig. 5. Cross-section of the nested tori in the $z = 0$ plane for system (5) with $a = 1$ and the surrounding chaotic sea.

return to the vicinity of the origin. This system is also unusual in that there are no equilibrium points, which ensures that all solutions oscillate endlessly.

The local divergence of this system is $(\frac{\partial \dot{x}}{\partial x} + \frac{\partial \dot{y}}{\partial y} + \frac{\partial \dot{z}}{\partial z} = z)$, and both solutions (quasi-periodic and chaotic) have $\langle z \rangle = 0$, which means the system is nonuniformly conservative. However, the vanishing of $\langle z \rangle$ cannot be discerned by a simple inspection of the equations as was the case for category B. The proof that the system is conservative relies on a nonobvious transformation of variables [Hoover *et al.*, 2016c] $x \to u$, $y \to v/s$, $z \to -w$, where s is a new time scaling variable conjugate to w and governed by $\dot{s} = ws$. The result is a four-dimensional uniformly conservative system with a Hamiltonian

$$H = \frac{1}{2}\left(su^2 + \frac{v^2}{s} + s\ln(s^2) + sw^2\right)$$

whose time derivative is zero provided $\dot{u} = \frac{v}{s}$, $\dot{v} = -us$, $\dot{w} = \frac{v^2}{s^2} - 1$, and $H = 0$ as one can verify [Dettmann & Morriss, 1997].

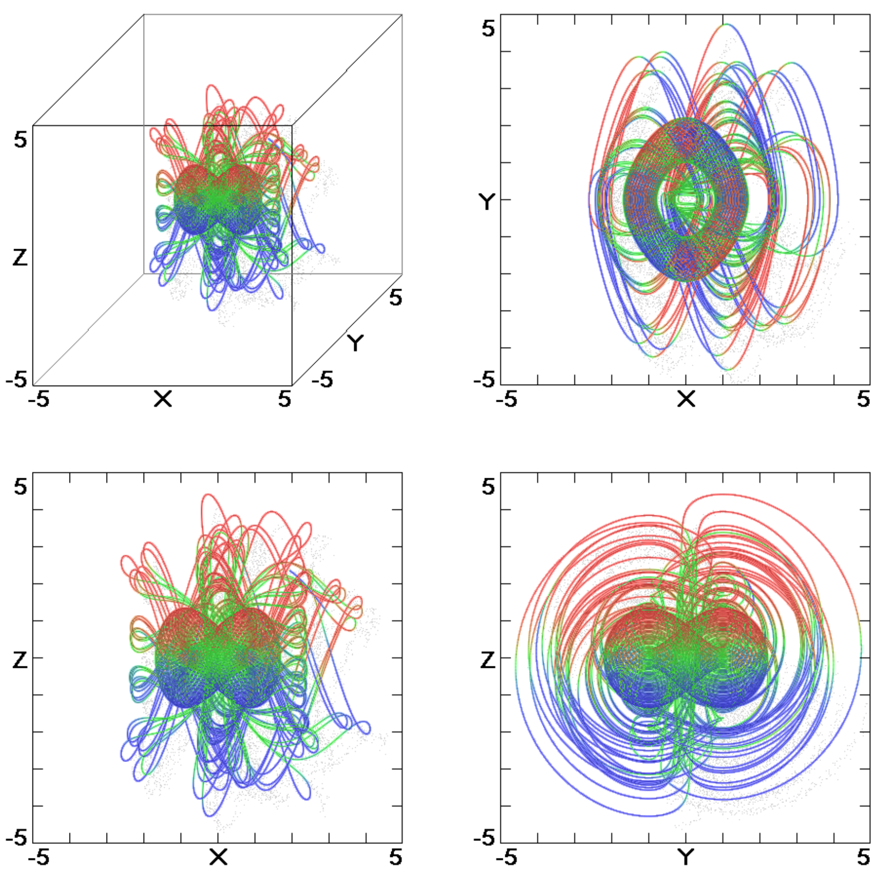

Fig. 6. Different projections of a typical torus for system (5) with $a = 1$ and initial conditions $(0, 1, 0)$ and the surrounding chaotic sea with initial conditions $(0, 5, 0)$.

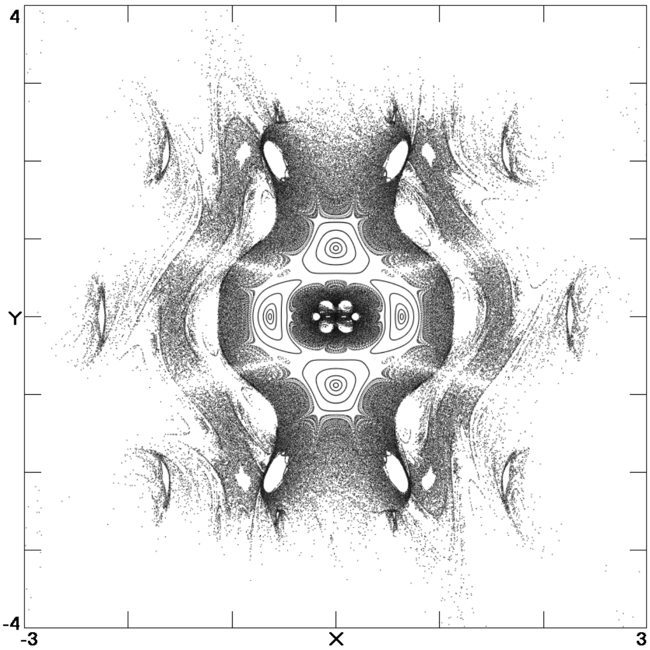

Fig. 7. Cross-section of the nested tori in the $z = 0$ plane for system (6) with $a = 4$ and $b = 1$ and the surrounding strange attractor.

2.4. *Category D*

One can modify system (5) by the addition of a term bx^2, analogous to the byz term that was added to system (3) to obtain system (4). Physically, this corresponds to assuming a temperature dependence that is a parabolic function of position x in the Nosé–Hoover oscillator, $\langle y^2 \rangle = \frac{1+x^2}{a}$. The resulting equations are

$$\dot{x} = y, \quad \dot{y} = -x + yz, \quad \dot{z} = 1 - ay^2 + bx^2. \tag{6}$$

This simple three-dimensional time-reversible system of ODEs with $a = 4$ and $b = 1$ has been introduced before [Sprott, 2015a] and has the unusual property that it exhibits conservative behavior for some initial conditions and dissipative behavior for others. The conservative regime has quasi-periodic orbits whose amplitude depends on the initial conditions, while the dissipative regime is chaotic. Thus a strange attractor coexists with an infinite set of nested invariant tori in the state space. Both solutions are time-reversible under the transformation

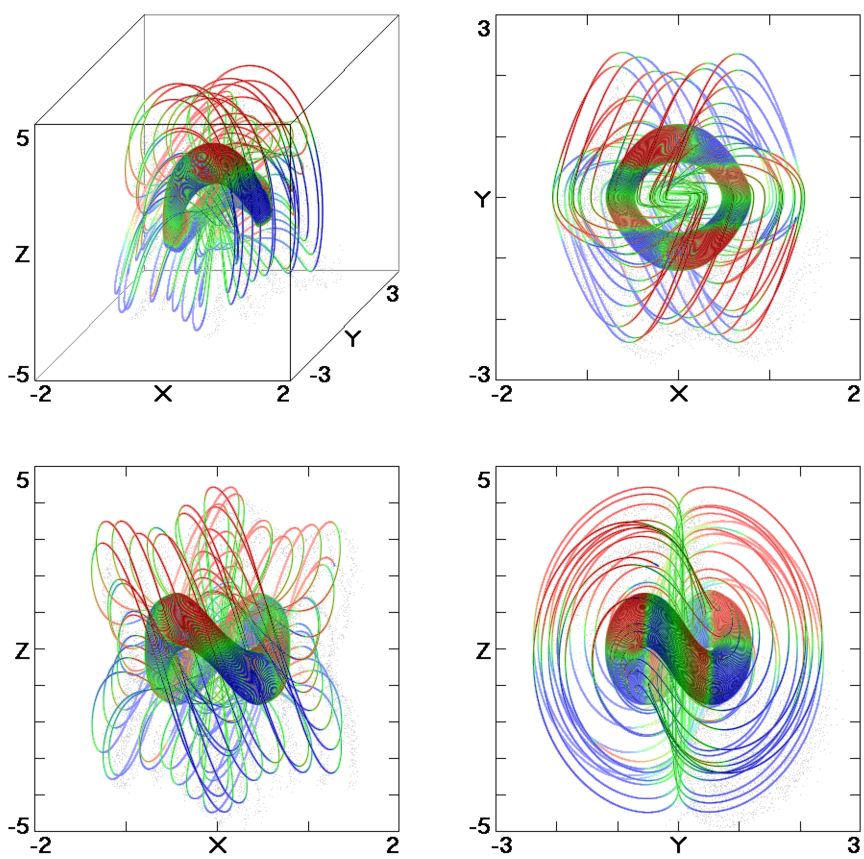

Fig. 8. Different projections of a typical torus for system (6) with $a = 4$ and $b = 1$ for initial conditions $(0, 2, 0)$ and the surrounding strange attractor with initial conditions $(1, 1.2, 0)$.

$(x, y, z, t) \rightarrow (x, -y, -z, -t)$, and the attractor has a corresponding repellor that becomes an attractor when time is reversed. The attractor is hidden in the sense that it cannot be found by starting from the vicinity of an equilibrium point since no such points exist for system (6).

The dissipation is given by the trace of the Jacobian matrix, $\mathrm{Tr}(J) = \langle z \rangle$. The surprise is that the time-average of z is negative (-0.0024) for some initial conditions such as $(0, 2, 0)$ and zero for others such as $(0, 1.2, 0)$. The first initial condition gives a strange attractor with Lyapunov exponents $(0.0131, 0, -0.0155)$ and a Kaplan–Yorke dimension of 2.8455, and the second initial condition gives a torus with Lyapunov exponents $(0, 0, 0)$ and a dimension of 2.0. Figure 7 shows a cross-section of the solutions in the $z = 0$ plane for various initial conditions, and Fig. 8 shows a typical torus with initial conditions $(0, 2, 0)$ surrounded by the strange attractor with initial conditions $(1, 1.2, 0)$.

We are aware of only two other examples of this type [Politi *et al.*, 1986; Sprott, 2014] plus variants of system (6) with different forms of the temperature gradient [Patra *et al.*, 2016], and we are unaware of any proof that they are conservative. Any such proof would require consideration of the initial conditions as well as the form of the equations.

3. Discussion and Conclusions

While we believe the examples given here may be the algebraically simplest 3D flows with quadratic nonlinearities for each of the four categories of conservative systems, we do not mean to imply that categories A and B can have only quasi-periodic solutions while categories C and D are always chaotic. Indeed, there are 3D category A chaotic systems such as Thomas labyrinth chaos [Thomas, 1999] and 4D category A chaotic systems such as the Hénon–Heiles system [Hénon & Heiles, 1964] as well as 3D category C systems that have no quasi-periodic solutions [Hoover *et al.*, 2016b]. Furthermore, replacing the bx^2 term in system (6) with bx leads to a system with a limit cycle that coexists with the conservative tori. The existence of category B chaotic systems and category C purely quasi-periodic systems remains an open question. Finally, we do not wish to imply that all category C systems have unbounded solutions, but only that boundedness is not required to prove that they are conservative. We have categorized some (and not all) dynamical systems published in literature in the Appendix.

In this note, we divided conservative flows into four categories. The first category is flows in which the dissipation is uniformly zero everywhere along the orbit. The second category is flows in which the dissipation depends on the state of the system and is zero on average as a simple consequence of the boundedness of the orbit and for which a simple proof exists. The third category is flows in which the dissipation depends on the state of the system and is zero on average, but the proof requires a transformation to a Hamiltonian system with the possible introduction of additional variables. The fourth category is flows in which the dissipation depends on the initial conditions and thus cannot be determined from the equations alone. Useful future work would entail cataloging the many known examples of conservative systems into these categories and looking for possible new categories and additional examples especially of categories B and D.

Conflicts of Interest

The authors declare no conflict of interest.

Acknowledgments

We thank Dr. Antonio Politi and Dr. Bill Hoover for help and comments which enhanced the quality of this paper.

References

Cang, S., Wu, A., Wang, Z. & Chen, Z. [2017] "Four-dimensional autonomous dynamical systems with conservative flows: Two-case study," *Nonlin. Dyn.* **89**, 2495–2508.

Dettmann, C. & Morriss, G. [1997] "Hamiltonian reformulation and pairing of Lyapunov exponents for Nosé–Hoover dynamics," *Phys. Rev. E* **55**, 3693.

Heidel, J. & Zhang, F. [2007] "Nonchaotic and chaotic behavior in three-dimensional quadratic systems: Five-one conservative cases," *Int. J. Bifurcation and Chaos* **17**, 2049–2072.

Hénon, M. & Heiles, C. [1964] "The applicability of the third integral of motion: Some numerical experiments," *Astron. J.* **69**, 73.

Hoover, W. G. [1995] "Remark on some simple chaotic flows," *Phys. Rev. E* **51**, 759.

Hoover, W. G., Hoover, C. G. & Sprott, J. C. [2016a] "Nonequilibrium systems: Hard disks and harmonic oscillators near and far from equilibrium," *Mol. Simul.* **42**, 1300–1316.

Hoover, W. G., Sprott, J. C. & Hoover, C. G. [2016b] "Ergodicity of a singly-thermostated harmonic oscillator," *Commun. Nonlin. Sci. Numer. Simul.* **32**, 234–240.

Hoover, W. G., Sprott, J. C. & Hoover, C. G. [2016c] "Adaptive Runge–Kutta integration for stiff systems: Comparing Nosé and Nosé–Hoover dynamics for the harmonic oscillator," *Amer. J. Phys.* **84**, 786–794.

Jafari, S., Sprott, J. C. & Golpayegani, S. M. R. H. [2016] "Layla and Majnun: A complex love story," *Nonlin. Dyn.* **83**, 615–622.

Li, C. & Sprott, J. [2014] "Chaotic flows with a single nonquadratic term," *Phys. Lett. A* **378**, 178–183.

Lichtenberg, A. J. & Lieberman, M. A. [2013] *Regular and Stochastic Motion*, Vol. 38 (Springer Science & Business Media).

Munmuangsaen, B., Sprott, J. C., Thio, W. J.-C., Buscarino, A. & Fortuna, L. [2015] "A simple chaotic flow with a continuously adjustable attractor dimension," *Int. J. Bifurcation and Chaos* **25**, 1530036-1–12.

Patra, P. K., Hoover, W. G., Hoover, C. G. & Sprott, J. C. [2016] "The equivalence of dissipation from Gibbs' entropy production with phase-volume loss in ergodic heat-conducting oscillators," *Int. J. Bifurcation and Chaos* **26**, 1650089-1–11.

Politi, A., Oppo, G. & Badii, R. [1986] "Coexistence of conservative and dissipative behavior in reversible dynamical systems," *Phys. Rev. A* **33**, 4055.

Posch, H. A., Hoover, W. G. & Vesely, F. J. [1986] "Canonical dynamics of the Nosé oscillator: Stability, order, and chaos," *Phys. Rev. A* **33**, 4253.

Sprott, J. C. [1994] "Some simple chaotic flows," *Phys. Rev. E* **50**, R647.

Sprott, J. [1997] "Some simple chaotic jerk functions," *Amer. J. Phys.* **65**, 537–543.

Sprott, J. C. & Chlouverakis, K. E. [2007] "Labyrinth chaos," *Int. J. Bifurcation and Chaos* **17**, 2097–2108.

Sprott, J. C. [2010] *Elegant Chaos: Algebraically Simple Chaotic Flows* (World Scientific, Singapore).

Sprott, J. [2014] "A dynamical system with a strange attractor and invariant tori," *Phys. Lett. A* **378**, 1361–1363.

Sprott, J. C., Hoover, W. G. & Hoover, C. G. [2014] "Heat conduction, and the lack thereof, in time-reversible dynamical systems: Generalized Nosé–Hoover oscillators with a temperature gradient," *Phys. Rev. E* **89**, 042914.

Sprott, J. [2015a] "Strange attractors with various equilibrium types," *Eur. Phys. J. Special Topics* **224**, 1409–1419.

Sprott, J. C. [2015b] "Symmetric time-reversible flows with a strange attractor," *Int. J. Bifurcation and Chaos* **25**, 1550078-1–7.

Thomas, R. [1999] "Deterministic chaos seen in terms of feedback circuits: Analysis, synthesis, 'labyrinth chaos'," *Int. J. Bifurcation and Chaos* **9**, 1889–1905.

Vaidyanathan, S. & Pakiriswamy, S. [2015] "A 3D novel conservative chaotic system and its generalized projective synchronization via adaptive control," *J. Engin. Sci. Technol. Rev.* **8**, 52–60.

Vaidyanathan, S. & Volos, C. [2015] "Analysis and adaptive control of a novel 3D conservative no-equilibrium chaotic system," *Arch. Contr. Sci.* **25**, 333–353.

Vaidyanathan, S. [2016a] "Anti-synchronization of novel coupled van der Pol conservative chaotic systems via adaptive control method," *Int. J. Pharm Tech Res.* **9**, 106–123.

Vaidyanathan, S. [2016b] "A novel 3D conservative jerk chaotic system with two quadratic nonlinearities and its adaptive control," *Advances in Chaos Theory and Intelligent Control* (Springer), pp. 349–376.

Vaidyanathan, S., Volos, C. *et al.* [2016] *Advances and Applications in Chaotic Systems*, Vol. 636 (Springer).

Appendix

Some examples of systems A, A & C, B, C, and D are given in Tables 1–5, respectively.

Table 1. Category A.

	System	Type	Chaos	Reference
1	$\dot{x} = z^2 + Ay$ $\dot{y} = x - z$ $\dot{z} = y$	A	•	[Heidel & Zhang, 2007]
2	$\dot{x} = yz + Ay$ $\dot{y} = \pm x + z$ $\dot{z} = x$	A	•	[Heidel & Zhang, 2007]

Table 1. (*Continued*)

	System	Type	Chaos	Reference
3	$\dot{x} = y + z$ $\dot{y} = -x + Az$ $\dot{z} = xy$	A	•	[Heidel & Zhang, 2007]
4	$\dot{x} = x + z$ $\dot{y} = -y + z$ $\dot{z} = xy$	A	•	[Heidel & Zhang, 2007]
5	$\dot{x} = y^2 - z + A$ $\dot{y} = z$ $\dot{z} = x$	A	•	[Heidel & Zhang, 2007]
6	$\dot{x} = z^2 + A$ $\dot{y} = x - z$ $\dot{z} = y$	A	•	[Heidel & Zhang, 2007]
7	$\dot{x} = yz + A$ $\dot{y} = x \pm z$ $\dot{z} = x$	A	•	[Sprott, 2010]
8	$\dot{x} = y$ $\dot{y} = z$ $\dot{z} = -ay - bx + \cos x - 1$	A	•	[Sprott, 2010]
9	$\dot{x} = y$ $\dot{y} = z$ $\dot{z} = -ay \pm (\lvert x\rvert - 1)$	A	•	[Sprott, 2010]
10	$\dot{x} = y$ $\dot{y} = z$ $\dot{z} = -ay \pm (x - x^3)$	A	•	[Sprott, 2010]
11	$\dot{x} = y$ $\dot{y} = z$ $\dot{z} = -ay \pm (x - \sin x)$	A	•	[Sprott, 2010]
12	$\dot{x} = y$ $\dot{y} = z$ $\dot{z} = -ay \pm x + x^2$	A	•	[Sprott, 2010]
13	$\dot{x} = y$ $\dot{y} = z$ $\dot{z} = -ay \pm bx - \cos x + 1$	A	•	[Sprott, 2010]
14	$\dot{x} = y$ $\dot{y} = z$ $\dot{z} = -y + x^2 - b$	A	•	[Sprott, 1997]

(*Continued*)

Table 1. (*Continued*)

	System	Type	Chaos	Reference
15	$\dot{x} = y$ $\dot{y} = z$ $\dot{z} = -x^2y + A(1 - x^2)x$	A	•	[Sprott, 1997]
16	$\dot{x} = y$ $\dot{y} = z$ $\dot{z} = -0.2x(1 - x) - y$	A	•	[Sprott, 1997]
17	$\dot{x} = y$ $\dot{y} = \sin 2z - x^3$ $\dot{z} = 1$	A	•	[Sprott, 2010]
18	$\dot{x} = y$ $\dot{y} = \sin 2z - x^5$ $\dot{z} = 1$	A	•	[Sprott, 2010]
19	$\dot{x} = y$ $\dot{y} = \sin 2z - x^7$ $\dot{z} = 1$	A	•	[Sprott, 2010]
20	$\dot{x} = y$ $\dot{y} = \sin 2z - x^9$ $\dot{z} = 1$	A	•	[Sprott, 2010]
21	$\dot{x} = y$ $\dot{y} = \sin 2z - x^{11}$ $\dot{z} = 1$	A	•	[Sprott, 2010]
22	$\dot{x} = y$ $\dot{y} = \sin 2z - \frac{x}{\sqrt{\lvert x \rvert}}$ $\dot{z} = 1$	A	•	[Sprott, 2010]
23	$\dot{x} = y$ $\dot{y} = \sin 2z - x\lvert x \rvert$ $\dot{z} = 1$	A	•	[Sprott, 2010]
24	$\dot{x} = y$ $\dot{y} = \sin z - x\lvert x \rvert^3$ $\dot{z} = 1$	A	•	[Sprott, 2010]
25	$\dot{x} = y$ $\dot{y} = \sin z - 0.2 \sin x$ $\dot{z} = 1$	A	•	[Sprott, 2010]
26	$\dot{x} = y$ $\dot{y} = \sin z - x + \tan x$ $\dot{z} = 1$	A	•	[Sprott, 2010]

Table 1. (*Continued*)

	System	Type	Chaos	Reference
27	$\dot{x} = y$ $\dot{y} = z$ $\dot{z} = -8y + \lvert x\rvert - 1$	A	•	[Sprott, 2010]
28	$\dot{x} = y$ $\dot{y} = z$ $\dot{z} = -4y + x(x^2 - 1)$	A	•	[Sprott, 2010]
29	$\dot{x} = y$ $\dot{y} = z$ $\dot{z} = -5y + 2x - \sin x$	A	•	[Sprott, 2010]
30	$\dot{x} = y$ $\dot{y} = z$ $\dot{z} = -9y + 3 - \cos x$	A	•	[Sprott, 2010]
31	$\dot{x} = v$ $\dot{v} = y - \sin x$ $\dot{y} = u$ $\dot{u} = -y$	A	•	[Sprott, 2010]
32	$\dot{x} = v$ $\dot{v} = y - \text{sgn}(x)$ $\dot{y} = u$ $\dot{u} = -\sin y$	A	•	[Sprott, 2010]
33	$\dot{x} = v$ $\dot{v} = y - x^3$ $\dot{y} = u$ $\dot{u} = -\sin y$	A	•	[Sprott, 2010]
34	$\dot{x} = v$ $\dot{v} = y - \sin x$ $\dot{y} = u$ $\dot{u} = -\sin y$	A	•	[Sprott, 2010]
35	$\dot{x} = v$ $\dot{v} = y \sin x$ $\dot{y} = u$ $\dot{u} = -\sin y$	A	•	[Sprott, 2010]
36	$\dot{x} = v$ $\dot{v} = y - \text{sgn}(x)$ $\dot{y} = u$ $\dot{u} = -\text{sgn}(y)$	A	•	[Sprott, 2010]

(*Continued*)

Table 1. (*Continued*)

	System	Type	Chaos	Reference
37	$\dot{x} = v$ $\dot{v} = y - x^3$ $\dot{y} = u$ $\dot{u} = -\mathrm{sgn}(y)$	A	•	[Sprott, 2010]
38	$\dot{x} = v$ $\dot{v} = y \sin x$ $\dot{y} = u$ $\dot{u} = -\mathrm{sgn}(y)$	A	•	[Sprott, 2010]
39	$\dot{x} = v$ $\dot{v} = y - \sin x$ $\dot{y} = u$ $\dot{u} = -y^3$	A	•	[Sprott, 2010]
40	$\dot{x} = v$ $\dot{v} = y - \mathrm{sgn}(x)$ $\dot{y} = u$ $\dot{u} = -y^3$	A	•	[Sprott, 2010]
41	$\dot{x} = v$ $\dot{v} = y - x^3$ $\dot{y} = u$ $\dot{u} = -y^3$	A	•	[Sprott, 2010]
42	$\dot{x} = v$ $\dot{v} = y \sin x$ $\dot{y} = u$ $\dot{u} = -y^3$	A	•	[Sprott, 2010]
43	$\dot{x} = v$ $\dot{v} = k(y - x) - \sin x$ $\dot{y} = u$ $\dot{u} = k(x - y) - \sin y$	A	•	[Sprott, 2010]
44	$\dot{x} = v$ $\dot{v} = y - x - \sin x$ $\dot{y} = u$ $\dot{u} = x - y - \mathrm{sgn}(y)$	A	•	[Sprott, 2010]
45	$\dot{x} = v$ $\dot{v} = y - x - \sin x$ $\dot{y} = u$ $\dot{u} = x - y - y^3$	A	•	[Sprott, 2010]

Table 1. (*Continued*)

	System	Type	Chaos	Reference
46	$\dot{x} = v$ $\dot{v} = y - x - \operatorname{sgn}(x)$ $\dot{y} = u$ $\dot{u} = x - y - \operatorname{sgn}(x)$	A	•	[Sprott, 2010]
47	$\dot{x} = v$ $\dot{v} = y - x - \operatorname{sgn}(x)$ $\dot{y} = u$ $\dot{u} = x - y - y^3$	A	•	[Sprott, 2010]
48	$\dot{x} = v$ $\dot{v} = y - x - x^3$ $\dot{y} = u$ $\dot{u} = x - y - y^3$	A	•	[Sprott, 2010]
49	$\dot{x} = v$ $\dot{v} = yx$ $\dot{y} = u$ $\dot{u} = -x^2 + 0.57y^2$	A	•	[Sprott, 2010]
50	$\dot{x} = v$ $\dot{v} = y$ $\dot{y} = u$ $\dot{u} = -(1 + \cos x)y - (1 - v^2)\sin x$	A	•	[Sprott, 2010]
51	$\dot{x} = v$ $\dot{v} = y$ $\dot{y} = u$ $\dot{u} = -6y + 1 - x^2$	A	•	[Sprott, 2010]
52	$\dot{x} = v$ $\dot{v} = y$ $\dot{y} = u$ $\dot{u} = -8y + v^2 - x$	A	•	[Sprott, 2010]
53	$\dot{x} = y$ $\dot{y} = z$ $\dot{z} = -y - x\left(\frac{x^2}{3} - c\right)$	A	•	[Sprott, 2010]
54	$\dot{x} = y$ $\dot{y} = z$ $\dot{z} = -ay + x(x^2 + y^2 - b)$	A	•	[Vaidyanathan *et al.*, 2016]
55	$\dot{x} = y$ $\dot{y} = z$ $\dot{z} = -0.2x(1 - x) - y + 0.01y^2$	A	•	[Vaidyanathan, 2016b]

(*Continued*)

Table 1. (*Continued*)

	System	Type	Chaos	Reference
56	$\dot{x} = y$ $\dot{v} = -x + 8.5(1 - x^2)w + 0.5z$ $\dot{z} = w$ $\dot{w} = -x + 8.5(1 - z^2)y + 0.5x$	A	•	[Vaidyanathan, 2016a]
57	$\dot{x} = yz$ $\dot{y} = xz$ $\dot{z} = -xy$	A		[Li & Sprott, 2014]
58	$\dot{x} = \sin y$ $\dot{y} = \sin z$ $\dot{z} = \sin x$	A	•	[Sprott & Chlouverakis, 2007]
59	$\dot{x} = \tan y$ $\dot{v} = \tan(z - x)$ $\dot{z} = \tan w$ $\dot{w} = \tan -z$	A	•	[Sprott, 2010]

Table 2. Categories A & C.

	System	Hamiltonian Function	Type	Chaos	Reference
60	$\dot{x} = \frac{y}{z^2}$ $\dot{v} = -x$ $\dot{z} = w$ $\dot{w} = \frac{y^2}{z^3} - \frac{1}{z}$	$H = \frac{1}{2}\left(x^2 + \frac{y^2}{z^2} + \ln(z^2) + w^2\right)$	A, C	•	[Hoover *et al.*, 2016a]
61	$\dot{x} = ayw$ $\dot{v} = xz$ $\dot{z} = -xy + bw$ $\dot{w} = -axy - bz$	$H = \frac{1}{2}(x^2 + y^2 + z^2 + w^2)$	A, C	•	[Cang *et al.*, 2017]
62	$\dot{x} = 1 + z^2 - w^2$ $\dot{v} = 2zw$ $\dot{z} = -1 + x^2 - y^2$ $\dot{w} = 2xy$	$H = L + \frac{L^3}{3} + M + \frac{M^3}{3}$ $L = x + iy$ $M = z + iw$	A, C	•	[Jafari *et al.*, 2016]
63	$\dot{x} = v + ku$ $\dot{v} = -x^3$ $\dot{y} = u + kv$ $\dot{u} = -y^3$	$H = \frac{1}{2}(v^2 + u^2) + \frac{1}{4}(x^4 + y^4) + kvu$	A, C	•	[Sprott, 2010]

Table 2. (*Continued*)

	System	Hamiltonian Function	Type	Chaos	Reference
64	$\dot{x} = v + kvu^2$ $\dot{v} = -x$ $\dot{y} = u + kuv^2$ $\dot{u} = -y$	$H = \frac{1}{2}(v^2 + u^2 + x^2 + y^2 + k(uv)^2)$	A, C	•	[Sprott, 2010]
65	$\dot{x} = v$ $\dot{v} = -(1 + ky^2)x$ $\dot{y} = u$ $\dot{u} = -(1 + kx^2)y$	$H = \frac{1}{2}(v^2 + u^2 + x^2 + y^2 + k(uv)^2)$	A,C	•	[Sprott, 2010]
66	$\dot{x} = 2v$ $\dot{v} = 2xy$ $\dot{y} = -2u$ $\dot{u} = 4y + x^2$	$H = v^2 - u^2 - 2y^2 - x^2y$	A, C	•	[Sprott, 2010]
67	$\dot{x} = v$ $\dot{v} = -x - 2xy$ $\dot{y} = u$ $\dot{u} = -y - x^2 + y^2$	$H = \frac{1}{2}(v^2 + u^2 + x^2 + y^2) + x^2y - \frac{1}{3}y^3$	A, C	•	[Sprott, 2010]

Table 3. Category B.

	System	Type	Chaos	Reference
68	$\dot{x} = y$ $\dot{y} = z$ $\dot{z} = -z^2 - x^2y - 0.25x$	B	•	[Heidel & Zhang, 2007]

Table 4. Category C.

	System	Hamiltonian Function	Type	Chaos	Reference
69	$\dot{x} = cyw$ $\dot{y} = yz$ $\dot{z} = -y^2 + dw$ $\dot{w} = -cxy - dz$	$H = \frac{1}{2}(x^2 + y^2 + z^2 + w^2)$	C	•	[Cang *et al.*, 2017]
70	$\dot{x} = \frac{y}{z}$ $\dot{y} = -zx$ $\dot{z} = zw$ $\dot{w} = \frac{y^2}{z^2} - 1$	$H = \frac{1}{2}\left(zx^2 + \frac{y^2}{z} + z\ln(z^2) + zw^2\right)$	C	•	[Dettmann & Morriss, 1997]

(*Continued*)

Table 4. (*Continued*)

	System	Hamiltonian Function	Type	Chaos	Reference
71	$\dot{x} = y$ $\dot{y} = -x + yz$ $\dot{z} = 5 - \lvert y \rvert$		C	•	[Munmuangsaen *et al.*, 2015]
72	$\dot{x} = y$ $\dot{y} = -x + yz$ $\dot{z} = 1 - x^4$		C	•	[Vaidyanathan & Pakiriswamy, 2015]
73	$\dot{x} = 0.05y + xz$ $\dot{y} = -x + yz$ $\dot{z} = 1 - x^2 - y^2$		C	•	[Vaidyanathan & Volos, 2015]

Table 5. Category D.

	System	Initial Condition	Type	Reference
74	$\dot{x} = y + 2xy + xz$ $\dot{y} = 1 - 2x^2 + yz$ $\dot{z} = x - x^2 - y^2$	$(1, 0, 0)$ (torus) $(2, 0, 0)$ (strange attractor)	D	[Sprott, 2014]
75	$\dot{x} = y$ $\dot{y} = -x - yz$ $\dot{z} = y^2 - 1 - 0.42 \tanh x$	$(-2.3, 0, 0)$ (torus) $(3.5, 0, 0)$ (torus) $(-2.7, 0, 0)$ (limit cycle)	D	[Sprott *et al.*, 2014]
76	$\dot{x} = -yz$ $\dot{y} = (2x + y + z^2)z$ $\dot{z} = x - x^3$	$(-1, -1.5, -0.5)$ (torus) $(-1, 0, -1)$ (strange attractor)	D	[Sprott, 2015b]